# Effects of quantum confinement and strain in $Zn_{1-x}Cd_xSe/ZnSe$ strained-layer superlattices



1995 J. Phys.: Condens. Matter 7 5835

(http://iopscience.iop.org/0953-8984/7/29/010)

J. Phys.: Condens. Matter 7 (1995) 5835–5842. Printed in the UK

# Effects of quantum confinement and strain in $Zn_{1-x}Cd_xSe/ZnSe$ strained-layer superlattices

J Wang†, Xun Wang†, Z Q Zhu‡§ and T Yao‡§

† Surface Physics Laboratory, Fudan University, Shanghai 200433, People's Republic of China

‡ Department of Electrical Engineering, Hiroshima University, Higashi-Hiroshima 724, Japan

Received 24 January 1995, in final form 23 March 1995

**Abstract.** The effects of strain and quantum confinement in $Zn_{1-x}Cd_xSe/ZnSe$ strained-layer superlattices grown by molecular beam epitaxy on the GaAs(100) substrates were studied using photoluminescence (PL) at 4.4 K. The sample with 30 periods and total thickness of 3600 Å was directly grown on the substrate without a buffer layer. The PL spectrum shows a single peak that is attributed to the free excitons between the lowest electron subband and ground heavy-hole subband of the $Zn_{1-x}Cd_xSe$ wells. The blue shifts of the excitonic peaks in the PL spectra induced by the effects of strain and quantum confinements were calculated on the basis of deformation potential theory and Bastard's method, respectively. In addition, the temperature dependence of the PL features of the sample was studied both theoretically and experimentally in detail. The experimental results coincide with the theoretical predictions very well.

## 1. Introduction

There is considerable interest in the wide-band-gap II–VI semiconductor quantum wells and superlattices, particularly in $Zn_{1-x}Cd_xSe/ZnSe$ quantum wells and superlattices, since the blue–green laser operations have been demonstrated recently by utilizing a $Zn_{1-x}Cd_xSe/ZnSe$ quantum well as the active layer [1–5]. For the applications of various optoelectronic devices of these materials, the studies of optical properties of $Zn_{1-x}Cd_xSe/ZnSe$ superlattices and quantum wells are very important in which the luminescent spectra are dominated by excitonic transitions involving the electron subbands and hole subbands induced by the effect of quantum confinement [6–12]. Unlike the case of $GaAs/Ga_xAl_{1-x}As$, where the heterolayers are basically lattice matched, the $Zn_{1-x}Cd_xSe/ZnSe$ heterolayers are under considerable strain owing to the lattice mismatch presented between them. The strain effect removes the degeneracy of valence bands, shifts the band-edge energies and induces the unique optical and electrical properties.

In this paper, the optical characteristics of $Zn_{1-x}Cd_xSe/ZnSe$ superlattices were studied by photoluminescence (PL) at 4.4 K. The single emitting peak in the PL spectrum is attributed to the free-exciton transitions between the lowest electron subband and the ground heavy-hole subband of the $Zn_{1-x}Cd_xSe$ well. The blue shifts of the excitonic peaks observed in PL spectra are contributed by the effects of the strain and the quantum confinement. The strain-induced effects on band structures were calculated with the equations developed for the III–V structure, and the confinement electron and hole energies were calculated by the

§ Present address: Institute for Materials Research, Tohoku University, 2-1-1 Katahira, Aoba-Ku, Sendai 980, Japan.

0953-8984/95/295835+08$19.50  

method derived by Bastard [9]. The temperature-dependence PL intensity, peak position and linewidth were also discussed. The temperature dependence of the linewidth is consistent with a broadening model in which the free excitons are scattered by the LO and TO phonons and ionized donor impurities.

## 2. Sample preparation and structural characterization

The $Zn_{0.77}Cd_{0.23}Se/ZnSe$ superlattice with 30 periods was grown by the molecular beam epitaxy (MBE) on (100)-oriented GaAs substrate at 250 °C with elemental sources Cd (purity, 99.9999% ), Se (purity, 99.9999% ) and Zn (purity, 99.9999% ). In order to determine the Cd contents, the $Zn_{1-x}Cd_xSe$ epilayers were grown first and $x$-values were calibrated from the results of x-ray diffraction (XRD) using Vegard's law and confirmed by the peak positions of PL spectra [13]. The layer thicknesses of superlattice were designed to be $L_w = L_b = 60$ Å by the growth rate and growth time and were calibrated by XRD and TEM. The results of XRD and TEM gave $L_w + L_b = 117$ Å which is very close to the expected layer thicknesses. Figure 1 shows an XRD spectrum of the superlattice sample. The several orders of well resolved satellite peaks in figure 1 correspond to the modulated structure with sharp interfaces.

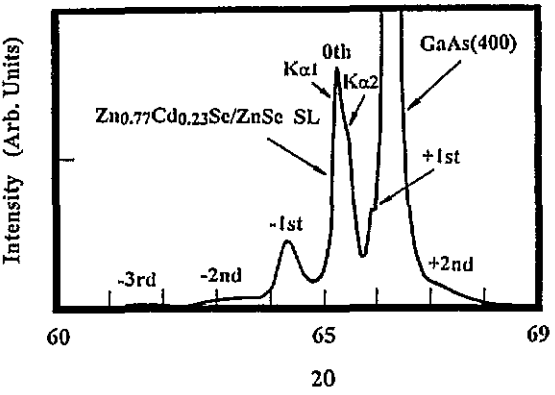


**Figure 1.** The XRD spectrum of the $Zn_{0.77}Cd_{0.23}Se/ZnSe$ superlattice.

If the total thickness of a strained-layer superlattice is substantially larger than a certain critical thickness, the superlattice would be expected to relax to its equilibrium lattice constant rather than to maintain the lattice constant of the substrate. In our case, the $Zn_{1-x}Cd_xSe/ZnSe$ superlattice ($x = 0.23$; $N = 30$; $L_w = 60$ Å; $L_b = 60$ Å) directly grown on the GaAs(100) substrate can be treated as a free-standing case because the total thickness (3600 Å) of the superlattice is larger than its critical thickness. The equilibrium in-plane lattice constant of the free-standing superlattice is give by [8, 14, 15].

$$a^{\parallel} = a_{ZnSe}[1 + f/(1 + G_{ZnSe}d_{ZnSe}/G_{Zn_{1-x}Cd_xSe}d_{Zn_{1-x}Cd_xSe})] \tag{1}$$

where $f$ is the lattice mismatch of ZnSe with respect to $Zn_{1-x}Cd_xSe$ given by $f = (a_{Zn_{1-x}Cd_xSe} - a_{ZnSe})/a_{ZnSe}$, $d_{ZnSe}$ and $d_{Zn_{1-x}Cd_xSe}$ are the layer thicknesses, $G_{ZnSe}$ and $G_{Zn_{1-x}Cd_xSe}$ are the shear moduli given by

$$Gi = 2[C^i_{11} + C^i_{12} - 2(C^i_{12})^2/C^i_{11}] \tag{2}$$

where $C_{11}^i$ and $C_{12}^i$ are the elastic stiffness constants. The mismatches between the lattice constant of the free-standing structure and those of the $Zn_{0.77}Cd_{0.23}Se$ well and ZnSe barrier are 0.86% and 0.80%, respectively, at room temperature. The thicknesses of the well and barrier layers should be controlled below their 'critical thickness $h_c$' to keep the layers in commensurate form. The values of the critical thicknesses are calculated by the energy model (EM) derived by Van de Leur *et al* [16]:

$$b[\ln(8\alpha R_c/b) - 2]/8R_c = \pi(1+\nu)\varepsilon/\sqrt{6}(2-\nu) \tag{3}$$

$$h_c = R_c\sqrt{\tfrac{2}{3}} \tag{4}$$

where $\varepsilon$ is the lattice mismatch $a_{Zn_{1-x}Cd_xSe}$ and $a''$, $b = 4$ Å is the Burgers vector, $\nu = 0.38$ is Poisson's ratio and $\alpha = 4$ is the core parameter.

In our case, the individual layer thicknesses (60 Å) of the $Zn_{0.77}Cd_{0.23}Se$ well and ZnSe barrier are well below the critical layer thicknesses of 253 Å and 276 Å predicted by the EM model [16]. In order to verify the validity of the EM model, we also use it to calculate the critical thickness of the $ZnSe/Zn_{0.82}Cd_{0.18}Se/ZnSe$ single quantum well. The calculated critical thickness is about 153 Å and below the experimental value of 240 Å [7]. Thus, the designed layer thickness of 60 Å in our $Zn_{0.77}Cd_{0.23}Se/ZnSe$ superlattice sample is well below the critical layer thickness. The free-standing superlattice structure is strained.

## 3. The photoluminescence spectra of the superlattice

Figure 2 shows a typical PL spectrum (curve A) of the $Zn_{0.77}Cd_{0.23}Se/ZnSe$ superlattice sample. For comparison, we have also introduced the spectrum (curve B) of a $Zn_{0.77}Cd_{0.23}$ epilayer grown on a GaAs(100) substrate. The spectra in figure 2 were measured at 4.4 K using the 325 nm line of a He–Cd laser with the power density of 10 mW $cm^{-2}$. The peak is 2.514 eV of curve B in figure 2 originates from the impurity bound excitons, which are about 10 meV below the band gap [13]. The peak at around 2.582 eV of curve A shows a clear blue shift compared with curve B. This peak behaves in an excitonic-like manner and it is more reasonable to attribute it to the free-exciton transitions between the lowest electron subband and the ground heavy-hole subband of $Zn_{0.77}Cd_{0.23}Se$ wells of the superlattice rather than to the bound excitons on impurities. The linewidth of the peak is about 28 meV which is slightly larger than the results obtained from the $Zn_{1-x}Cd_xSe/ZnSe$ single quantum wells [6–7].

Figure 3 shows the temperature dependence of the PL peak energy of the superlattice sample, with the open squares denoting experimental data and the solid curve indicating a theoretical fit to empirical data using Varshni's [17] formula [6]:

$$E(T) = E(0\text{ K}) - \alpha T^2/(T+\beta) \tag{5}$$

where $E(0\text{ K}) = 2.582$ eV, $\alpha = -4 \times 10^{-4}$ and $\beta = -520$ K. The theoretical calculations are in good agreement with the experimental data. Although equation (5) holds for the band gap $E_g$, the PL peak energy might follow the same relation at low temperatures, if we assume that the peaks are due to the excitonic transitions.

Figure 4 shows the temperature dependence of the linewidth of the PL peak. The temperature dependence of the emission linewidth for the heavy-hole exciton can be analysed by the following equation [6, 10, 18, 19]:

$$\Gamma_{total} = \Gamma_0^+ + \Gamma T + \Gamma_{LO}[\exp(E_{LO}/kT) - 1]^{-1} + \Gamma_{imp}\exp(-(E)/kT). \tag{6}$$

the first term $\Gamma_0^+$ is the linewidth due to inhomogeneous origin. Three predominant mechanisms of inhomogeneous broadening are of relevance here:

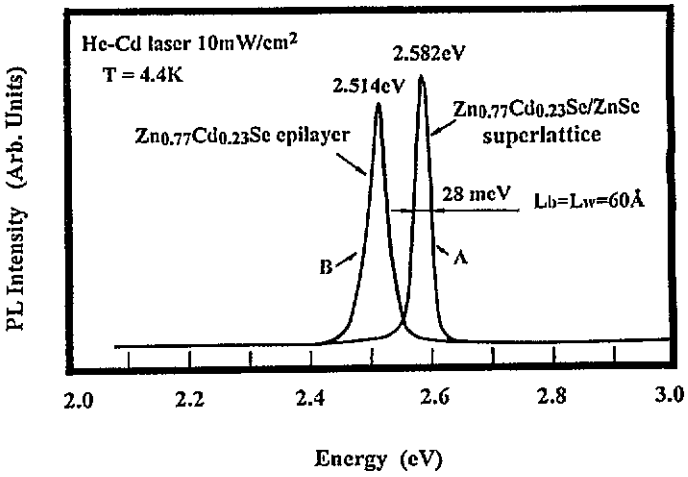


**Figure 2.** The PL spectra of the $Zn_{0.77}Cd_{0.23}Se/ZnSe$ superlattice and $Zn_{0.77}Cd_{0.23}Se$ epilayer at $T = 4.4$ K.

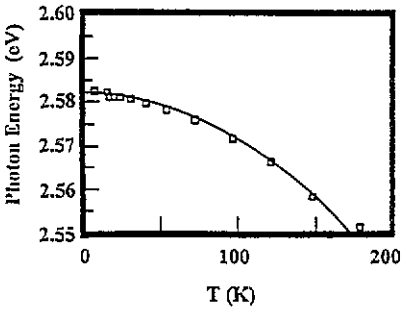


**Figure 3.** The temperature dependence of the free-exciton energy of the $Zn_{0.77}Cd_{0.23}Se/ZnSe$ superlattice: □, experimental data; ——, theoretical fit.

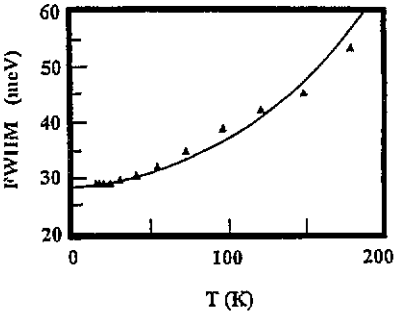


**Figure 4.** The temperature dependence of linewidth (FWHM) of the free-exciton emission of the $Zn_{0.77}Cd_{0.23}Se/ZnSe$ superlattice: ——, fit to equation (4); ▲, experimental data.

(i) alloy concentration fluctuation;
(ii) monolayer-type interface roughness;
(iii) fluctuation of well thicknesses.

The second term is the interaction between excitons and acoustic phonons via deformation and the piezoelectric potential $\Gamma$. The interaction $\Gamma_{LO}$ of excitons with polar optical phonons is described by the third term, in which, by absorbing one LO phonon of energy $\hbar\omega$ via the Frohlich interaction, a 1S ($q = 0$) exciton either dissociates into the free electron–hole continuum or scatters within the discrete bands. It is important to note that the former process requires that the exciton binding energy is smaller than $\hbar\omega_{LO}$. The last term $\Gamma_{imp}$ is caused by the ionized-impurity scattering and $\langle E \rangle$ is the average binding energy of the donors.

Fitting the above equation to our data yields the solid curve in figure 4 with the parameters $\Gamma_0^+ = 28$ meV, $\Gamma = 4 \times 10^{-5}$ eV $K^{-1}$, $\Gamma_{LO} = 38$ meV, $E_{LO} = 30.4$ meV, $\Gamma_{imp} = 80$ meV and the donor binding energy $\langle E \rangle = 25$ meV. At low temperatures, the

acoustic phonon scattering is the dominant mechanism for broadening the FWHM. When $T$ is larger than 100 K, ionized-impurity scattering begins to make a significant contribution to the FWHM. However, the polar optical phonon scattering has the smallest effect on broadening the FWHM compared with acoustic phonon scattering and ionized-impurity scattering at $0\ \text{K} \leqslant T \leqslant 200\ \text{K}$. This is because the exciton binding energy of the superlattice with narrow quantum wells becomes larger, even larger than the LO-phonon energy, so that the dissociation channel absorption is inhibited, resulting in an effective reduction in $\Gamma_{LO}$ ($\Gamma_{LO} = 60$ for bulk ZnSe).

Figure 5 shows the temperature dependence of the PL intensity of the superlattice sample. The PL quenched at higher temperatures is mainly due to the thermally activated non-radiative recombination channels. The activation energy obtained from figure 5 is about 41 meV.

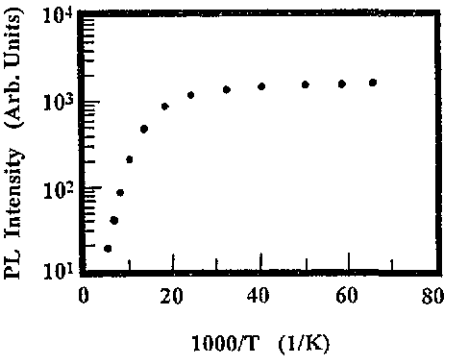


**Figure 5.** The temperature dependence of the PL intensity of the $Zn_{0.77}Cd_{0.23}Se/ZnSe$ superlattice: ●, experimental data.

## 4. Theoretical calculations on the effects of strain and quantum confinement

Based on Hill's theory [6, 7, 19], the band gap varies with $x$ according to

$$E_g(x) = E_{gCdSe} + (E_{gZnSe} - E_{gCdSe} - b)(1 - x) + b(1 - x)^2 \tag{7}$$

where $b$ is the bowing parameter. According to [6], we take $b = 0.301$, $E_{gZnSe} = 2.821$ eV and $E_{gCdSe}(ZB) = 1.765$ eV; equation (7) gives $E_g = 2.525$ eV for $x = 0.23$ at 10 K. By comparison with the value calculated from equation (7), the peak position (2.582 eV) of the $Zn_{0.77}Cd_{0.23}Se/ZnSe$ superlattice has a clear blue shift, which is attributed to the effects of mismatched strain and quantum confinement as described earlier.

In this section, we present theoretical calculations for the confined-carrier energies in the $Zn_{0.77}Cd_{0.23}Se$ well and for the effect of strain on the transition energies of the $Zn_{1-x}Cd_xSe/ZnSe$ free-standing superlattices with equal thicknesses of the well and barrier. The goal is to obtain a good fit to the experimental data of luminescent transitions.

If we define that the $z$ direction is along the growth direction, then the elastic strains $\varepsilon_{ij}$, corresponding to the $Zn_{1-x}Cd_xSe$ layers, are given by

$$\varepsilon_{xx} = \varepsilon_{yy} = \varepsilon = (a_{Zn_{1-x}Cd_xSe} - a'')/a'' \tag{8}$$

$$\varepsilon_{zz} = -2C_{12}\varepsilon_{xx}/C_{11} \tag{9}$$

$$\varepsilon_{xy} = \varepsilon_{yx} = \varepsilon_{zx} = 0 \tag{10}$$

**Table 1.** Lattice constants $a$, elastic constants $C_{ij}$, hydrostatic deformation potentials $e$ and shear deformation potentials $b$.

| | $a$ (Å) | $C_{11}$ ($10^{10}$ N m$^{-2}$) | $C_{12}$ ($10^{10}$ N m$^{-2}$) | $e$ (eV) | $b$ (eV) |
|---|---|---|---|---|---|
| ZnSe(ZB) | 5.6676 | 8.26 | 4.98 | −4.25 | −1.20 |
| CdSe(ZB) | 6.077 | 6.67 | 4.63 | −3.66 | −0.80 |
| $Zn_{0.77}Cd_{0.23}Se$(ZB) | 5.7617 | 7.89 | 4.90 | −4.11 | −1.11 |

where $a''$ is the equilibrium lattice constant of the superlattice in the free-standing case. For the zincblende-type material, the valence bands at $k = 0$ consist of a fourfold $P_{3/2}$ multiplet ($j = \frac{3}{2}$; $m_j = \pm\frac{3}{2}, \pm\frac{1}{2}$) and a twofold $P_{1/2}$ multiplet ($j = \frac{1}{2}$; $m_j = \pm\frac{1}{2}$). For the case of biaxial in-plane compression, the $P_{3/2}$ valence band splits because of lowering the symmetry from $T_d$ to $D_{2d}$. In addition, the hydrostatic component of the stress shifts the centre of gravity of the $P_{3/2}$ and $P_{1/2}$ multiplets relative to the bottom of the lowest conduction band and may also influence the relative line-ups and thus the band discontinuities between the two materials [6, 15]. Pikus and Bir [20] have reported that the orbital strain Hamiltonian for a given band at $k = 0$ can be written as

$$H\varepsilon = -e(\varepsilon_{xx} + \varepsilon_{yy} + \varepsilon_{zz}) - 3b[(L_x^2 - L^2/3)\varepsilon_{xx} + \text{CP}] - \sqrt{3}d[(L_x, L_y)\varepsilon_{xy} + \text{CP}] \tag{11}$$

where $L$ denotes the angular momentum operator, CP denotes the cyclic permutation with respect to the indices $x$, $y$ and $z$, and $(L_x, L_y)$ indicate the symmetrized product $(L_xL_y + L_yL_x)/2$. The parameter $e$ is the hydrostatic deformation potential. The quantities $b$ and $d$ are the shear deformation potentials appropriate to the strain of tetragonal and rhombohedral symmetries, respectively.

For the biaxial stress parallel to [100], the strain Hamiltonian $H\varepsilon$, thus, becomes

$$H\varepsilon = -2a[(C_{11} - C_{12})/C_{11}]\varepsilon_{xx} + 3b[(C_{11} + 2C_{12})/C_{11}](L_x^2 - L^2/3)\varepsilon_{xx} \tag{12}$$

where the first term represents the shift in the centre of gravity of $P_{3/2}$ and the second term describes the splitting of $P_{3/2}$ due to tetragonal distortion. The eigenvalues of the strain Hamiltonian can be calculated by using the unperturbed wavefunctions of the valence and conduction bands in a zincblende-type material. The increase in the band gap due to uniaxial compression is given by

$$\Delta E_0(1) = E_H + E_U \tag{13}$$

$$\Delta E_0(2) = E_H + (\Delta - E_U)/2 - [(9E_H^2 + 2\Delta E_U + \Delta^2)^{1/2}]/2 \tag{14}$$

where

$$E_H = -2e[(C_{11} - C_{12})/C_{11}]\varepsilon_{xx} \tag{15}$$

$$E_U = b[(C_{11} + 2C_{12})/C_{11}]\varepsilon_{xx} \tag{16}$$

and $\Delta = 0.43$ eV is the spin–orbit splitting [15]. Here, since it is difficult to obtain $\Delta$ for $Zn_{0.77}Cd_{0.23}Se$ or CdSe, we use $\Delta$, for ZnSe as an approximation for $\Delta$ for $Zn_{0.77}Cd_{0.23}Se$.

Taking the parameters from table 1 and interpolating linearly that for $Zn_{0.77}Cd_{0.23}Se$, the shifts of the heavy hole and light hole are

$$\Delta E_0(1) = 5.4 \text{ meV}$$

$$\Delta E_0(2) = 46.0 \text{ meV}$$

respectively.

In addition to the strain-induced renormalization of the energy bands, the electron and hole confinements also cause the transition energy to move to higher energies. This blue shift is a function of the band offsets and effective masses of the carriers involved. The confinement energies are calculated by solving numericlly the dispersion relation [9, 13, 15]:

$$\cos(KL) = \cos(k_a l_a)\cosh(k_b l_b) + \tfrac{1}{2}(x - 1/x)\sin(k_a l_a)\sinh(k_b l_b) \qquad (17)$$

where $L$ is the superlattice period $l_a + l_b$, $l_a$ and $l_b$ are the well and barrier widths and

$$x = k_b m_a / k_a m_b \qquad hk_a = (2m_a E)^{1/2} \qquad hk_b = [2m_b(V - E)]^{1/2}$$

where $m_a$ and $m_b$ are the effective masses in the well and barrier layers and $V$ is the potential barrier height corresponding to valence and conduction band offsets.

The valence and conduction band offsets for the CdSe/ZnSe heterostructure were calculated using the Harrison atomic-like orbital theory and those for the $Zn_{0.77}Cd_{0.23}Se/ZnSe$ system were linearly extrapolated to obtain $V_1 = 53$ meV for the valence band offset and $V_2 = 226$ meV for the conduction band offset [6, 7, 21, 22]. Considering the effect of strain, we obtain $\Delta E_v = V_1 + \Delta E_0(1) = 58.4$ meV and $\Delta E_c = V_2 = 226$ meV. By taking the effective masses and potential depths of $\Delta E_v$ and $\Delta E_c$ listed in table 2, the ground-state electron energy $E_{1e}$ and heavy-hole confinement energy $E_{1hh}$ are calculated by solving numerically equation (17), and they are about 41.5 meV and 18.2 meV, respectively. The final expression for the ground-state level $E_{th}$ of the heavy-hole excitonic transition can be written as

$$E_{th} = E_g + E_{1e} + E_{1hh} + \Delta E_0(1) - E_{ex} = 2.578 \text{ eV} \qquad (18)$$

where $E_{ex}$ is the binding energy of the free exciton. The free-exciton binding energies of bulk ZnSe and CdSe are 18 meV ad 15 meV, respectively, and that of $Zn_{1-x}Cd_xSe$ is interpolated as 17 meV. Here, we used free-exciton binding energies of bulk as an approximation for that of the superlattice [6–7]. The resultant $E_{th} = 2.578$ eV of the calculated values is in good agreement with the experimental result $E_{expt} = 2.582$ eV, which provides indirect evidence that the asumption of free-exciton transition is acceptable.

**Table 2.** Constants used in confined energy calculations.

| | $E_g$ (9 K) (eV) | $m_e$ ($m_0$) | $m_h$ ($m_0$) | $\Delta E_c$ (meV) | $\Delta E_v$ (meV) |
|---|---|---|---|---|---|
| ZnSe | 2.821 | 0.16 | 0.6 | | |
| CdSe | 1.765 | 0.13 | 0.45 | | |
| $Zn_{0.77}Cd_{0.23}Se$ | 2.524 | 0.153 | 0.566 | 226 | 58.4 |

## 5. Conclusion

The optical characterization of a $Zn_{0.77}Cd_{0.23}Se/ZnSe$ strained-layer superlattice was studied by the PL. The blue shifts of the excitonic peaks are considered as the effects of the quantum confinement and the strain. We have presented theoretical calculations for the confined-carrier energies in the $Zn_{1-x}Cd_xSe$ well and for the strain effect on the energy transitions

of the free-standing superlattices with equal thicknesses of well and barrier. The result is in good agreement with the experimental observation, which illustrates that the assignment of PL peak to the luminescence of free excitons is a reasonable expectation. The temperature dependence of the PL emission peak position, intensity and linewidth (FWHM) have also been analysed. The temperature dependence of the linewidth of the exciton luminescence has been explained by a broadening model in which the free excitons interact with LO and TO phonons and ionized donor impurities. The activation energy corresponding to the dissociation of the excitons is 41 meV.

## References


[1] Haase M A, Qiu J, DePuydt J M and Cheng H 1991 *Appl. Phys. Lett.* **59** 1272
[2] Jeon H, Ding J, Patterson W, Nurmikko A V, Xie W, Grillo D C, Kobayashi M and Gunshor R L 1991 *Appl. Phys. Lett.* **59** 3619
[3] Gaines J M, Drenten R R, Haberern K W, Marshall T, Mensz P and Petruzzello J 1993 *Appl. Phys. Lett.* **62** 2462
[4] Bhargava R N 1992 *Optoelectronic. Devices Technol.* **7** 19
[5] Nurmikko A V and Gunshor R L 1994 *IEEE J. Quantum Electron* **QE-30** 619
[6] Lozykowski H J and Shastri V K 1991 *J. Appl. Phys.* **69** 3235
[7] Ohki A, Ando K and Zembutsu S 1993 *J. Electron. Mater.* **22** 529
[8] Mohammed K, Olego D J, Newbury P, Cammack D A, Dalby R and Cornelissen H 1987 *Appl. Phys. Lett.* **50** 1820
[9] Bastard G 1981 *Phys. Rev.* B **24** 5693
[10] Pelekanos N T, Ding J, Hagerott M, Nurmikko A V, Luo H, Samarth N and Furdyna J K 1992 *Phys. Rev.* B **45** 6037
[11] Ding J, Pelekanos N, Nurmikko A V, Luo H, Samarth N and Furdyna J K 1990 *Appl. Phys. Lett.* **57** 2885
[12] Alonso R G, Parks C, Ramdas A K, Luo H, Samarth N, Furdyna J K and Ram-Mohan L R 1992 *Phys. Rev.* B **45** 1181
[13] Samarth N, Luo H, Furdyna J K, Alonso R G, Lee Y R, Ramdas A K, Qadri S B and Otsuka N 1990 *Appl. Phys. Lett.* **56** 1163
[14] People R 1986 *IEEE J. Quantum Electron.* **QE-22** 1696
[15] Shahzad K, Olego D J and Van de Welle C G 1988 *Phys. Rev.* B **38** 1417
[16] van de Leur R H M, Schellingerhcut A J G, Tuinstra F and Mooij J E 1988 *J. Appl. Phys.* **64** 3043
[17] Varshni Y P 1967 *Physica* **34** 149
[18] Lee J, Koteles E S and Vassell M O 1986 *Phys. Rev.* B **33** 5512
[19] Li T, Lozykowski H J and Reno J L 1992 *Phys. Rev.* B **46** 6961
[20] Pikus G E and Bir G L 1959 *Fiz. Tverd. Tela* **1** 1642 (Engl. Transl. 1959 *Sov. Phys.–Solid State* **1** 1502)
[21] Frensley W R and Kroemer H 1977 *Phys. Rev.* B **16** 2642
[22] Kroemer H 1985 *Molecular Beam Epitaxy (NATO ASI Series E 87)* ed L L Chang and K Ploog (Dordrecht: Martinus Nijhoff) p 33 and references therein